A low cost and highly efficient adsorbent (activated carbon) prepared from waste potato residue

Article *in* Journal of the Taiwan Institute of Chemical Engineers · December 2014

DOI: 10.1016/j.jtice.2014.11.024

CITATIONS
41

READS
268

7 authors, including:

Xinsheng Luo
Harbin Institute of Technology
33 PUBLICATIONS **516** CITATIONS
SEE PROFILE

Peng-Xin Zhou
The Northwest Normal University
25 PUBLICATIONS **435** CITATIONS
SEE PROFILE

Guofu Ma
The Northwest Normal University
102 PUBLICATIONS **3,060** CITATIONS
SEE PROFILE

Ziqiang Lei
The Northwest Normal University
447 PUBLICATIONS **10,271** CITATIONS
SEE PROFILE

Journal of the Taiwan Institute of Chemical Engineers 49 (2015) 206–211

Contents lists available at ScienceDirect

Journal of the Taiwan Institute of Chemical Engineers

journal homepage: www.elsevier.com/locate/jtice

A low cost and highly efficient adsorbent (activated carbon) prepared from waste potato residue

Zhe Zhang [a], Xinsheng Luo [a], Yani Liu [b], Pengxin Zhou [a], Guofu Ma [a], Ziqiang Lei [a,*], Lei Lei [a]

[a] Key Laboratory of Eco-Environment-Related Polymer Materials of Ministry of Education, Key Laboratory of Polymer Materials of Gansu Province, College of Chemistry and Chemical Engineering, Northwest Normal University, Lanzhou 730070, China
[b] College of Science, Gansu Agricultural University, Lanzhou 730070, China

ARTICLE INFO

Article history:
Received 16 August 2014
Revised 25 November 2014
Accepted 30 November 2014
Available online 20 December 2014

Keywords:
Adsorbent
Activated carbon
Waste potato residue
Methylene blue

ABSTRACT

This study was conducted to prepare a low cost and highly efficient adsorbent (activated carbon) from potato residue. The influence of the activation parameters such as carbonization temperatures and the impregnation ratios was investigated. The activated carbon (AC) was essentially mesoporous under the optimized conditions. The BET surface area, total pore volume and mesopore volume were as high as 1357 m^2/g, 1.065 cm^3/g and 0.982 cm^3/g, respectively. The properties of the carbon samples that were prepared under oxygen-limited conditions and N_2-atmosphere conditions were compared. The AC was used to adsorb methylene blue (q_e = 540 mg/g), and the results showed that the prepared AC is an effective adsorbent for the removal of the organic dye. The experimental results indicated that the use of potato residue as a precursor material for the preparation of AC was feasible.

1. Introduction

Activated carbon (AC) is a highly porous material which is the most widely used adsorbent [1] for removal of dyes, metal ions, and other organic compounds of low molar mass in water, due to its high adsorption capacity and fast removal rate. As the water pollution become more and more serious, the demand for AC is growing annually. However, commercial AC is relatively expensive and hampered its wide application in wastewater treatment. Therefore, to seek low cost adsorbents is still an attractive goal for chemists.

Currently, biomass agricultural waste materials such as rice husks [2], rice straw [3], waste tea [4], olive waste [5], coffee husks [6], barley husks [7], forest industries waste materials such as sawdust [8], fibers [9], switchgrass [10], bamboo culms [11], and agricultural-industries waste such as oil palm shell [12] *etc.* were used as raw materials for preparing AC, because these materials possess high carbon contents and are low in cost [13].

Potato residue mainly consists of starch, cellulose, hemicellulose and pectin (Table 1). It is one of the most undesired waste materials during starch production from potato. For example, in the Gansu province of China, the starch production processing cycle generates approximately 300,000 tons of potato residue and 2 million cubic meters of wastewater each year, but they are currently disposed of inadequately and has caused serious environmental pollution for soil, water and air (Fig. 1). Only a portion of the potato residue is used for limited practical applications, such as for the raw material in the production of solid fuel [14], a feedstock to obtain chemical compounds, or as a dietary-fiber additive in low-fat sausages [15]. To the best of our knowledge, the production of AC from potato residue has been paid little attention. If potato residue were used to produce AC, not only resolve the problem of environmental pollution caused by potato residue, which was produced during the starch production, but also afford a low cost adsorbent.

In this study, AC was prepared from waste potato residue with $ZnCl_2$ as an activating agent under either oxygen-limited (OL) conditions or N_2-atmosphere (NA) conditions. Two types of ACs were characterized by ultimate analysis, porosity analysis, TG/DTG, XRD, FT-IR, ξ-potential and SEM. The adsorption capacity of the two types of ACs was evaluated by the well-known probe dye molecule methylene blue (MB).

2. Materials and methods

2.1. Materials

Potato residue was collected from the Huining County, Gansu province, China. It was air-dried at room temperature and ground to pass through 80-mesh sieves, labeled DPR. $ZnCl_2$ was analytical, reagent grade from Yantai Shuangshuang Co., Ltd. Methylene blue ($C_{16}H_{18}ClN_3S_2 \cdot 3H_2O$) was purchased from Shanghai Zhongqin

* Corresponding author at: 967 Anning East Road, Lanzhou 730070, PR China. Tel.: +86 931 7971261.
E-mail address: nuli518@126.com (Z. Lei).

http://dx.doi.org/10.1016/j.jtice.2014.11.024
1876-1070/

Fig. 1. Pollution of potato residue.

Table 1
Components and ultimate analyses.

	DPR (wt.%)	AC-7 (wt.%)	AC-10 (wt.%)
Components analyses[a]			
Starch	37		
Cellulose	17		
Hemicellulose	14		
Pectin	17		
Fiber (unidentified)	7		
Protein/amino acids	4		
Ashes	4		
Ultimate analyses			
C	40.81	69.86	76.72
H	5.87	1.34	1.24
N	1.16	2.77	2.43
S	0.12	0.25	0.41
O[b]	52.04	25.78	19.20

[a] The study was from Frank Mayer [16].
[b] By difference.

Chemical Reagent Co., Ltd. Table 1 listed the components analysis of the DPR used in the study by Frank Mayer [16]. The ultimate analysis of the DPR and ACs was also showed in Table 1.

2.2. Preparation of the activated carbon

The DPR was mixed with $ZnCl_2$ solutions (50 wt.%) and kneaded. This mixture was then maintained at room temperature for 24 h to prepare the impregnated samples. Next, the impregnated samples were loaded into ceramic crucibles, each covered with a fitted lid, and pyrolyzed in a muffle furnace (OL conditions) [17] at a heating rate of 10 °C/min. The heating time at the maximum heat-treatment temperature was 1 h. ACs were prepared by maintaining the $ZnCl_2$:DPR ratio (*i.e.*, 100% by weight) and by varying the carbonization temperature between 400 and 800 °C (labeled AC-1, AC-2, AC-3, AC-4 and AC-5, respectively) or vice versa (varying $ZnCl_2$:DPR ratios of 50%, 150%, 200% and 250% at a steady temperature of 600 °C; labeled AC-6, AC-7, AC-8 and AC-9, respectively). For comparison, a sample with an impregnation ratio of 150% and an activation temperature of 600 °C was prepared under NA and labeled AC-10. After cooling, the samples were soaked in HCl solution (5%), and then were repeatedly washed with distilled water until the pH of the filtrate reached 6.5–7. Next, the samples were dried at 110 °C for 24 h in a vacuum drying oven. Finally, the samples were ground and stored in a valve bag. The activated carbon yield was defined as the final weight of the product after activation, washing, and drying. The percent yield (W) was determined from the relation:

$$W = (W_c/W_o) \times 100\%,$$

where W_c and W_o are the weight of the final activated-carbon product (g) and the weight of the DPR (g), respectively.

2.3. Textural and chemical characterization

The ultimate analysis of the DPR, AC-7 and AC-10 was determined on an organic elemental analyzer (Thermo Scientific Flash 2000). The samples were characterized in terms of the specific surface area, pore volume, and pore diameter using the adsorption of nitrogen (Micromeritics, TRISTARII3020) at 77 K. The surface area, S_{BET}, was determined from isotherms using the Brunauer–Emmett–Teller (BET) equation [18]. The single-point total pore volume, V_T, was determined from the amount of adsorbed nitrogen expressed in liquid form at a relative pressure of approximately 0.99. The micropore volume, V_{mi}, calculated by using the *t*-Plot micropore volume and the mesopore volume, V_{me}, was calculated as the difference between V_T and V_{me}. The average pore diameter, D_p, was calculated using the relation $4VT/S_{BET}$ and the pore-size distribution by the BJH method [19]. This study assumes that micropores are less than 2 nm wide, mesopores are 2–50 nm wide, and macropores are more than 50 nm wide [20]. The thermal behavior of the DPR was evaluated using a thermogravimetric analyzer (Perkin Elmer TG/DTA 6300) under N_2 gas flow at a heating rate of 10 °C/min. The crystalline structures of the DPR and AC were examined by an X-ray diffractometer (Rigaku, D/Max-2400) using Cu-Kα radiation with a scan speed of 10 °C/min. Fourier transform infrared (FTIR) spectra were also obtained using a spectrometer to determine the composition of the samples (Nicolet Nexus 670). The morphologies of the DPR and the AC were examined by field-emission scanning electron microscopy (FE-SEM, ZEISS ULTRA plus). The zeta potential values were determined on a zeta potential instrument (Malvern NANO ZEN 3600).

2.4. Adsorption tests

The AC was used in adsorption tests of aqueous MB solutions. Batch adsorption was performed in a set of 50-mL conical flasks containing 15 mL of MB solutions with various initial concentrations (100–600 mg/L). First, 15 mg of AC was added to each flask and kept at 30 °C on a shaker. For equilibrium studies, the experiment was performed over 3 h to ensure that equilibrium was reached. The collected supernatants were analyzed by UV–vis spectroscopy (PERSEE TU-1901 UV), analyzing the MB peak wavelength of 664 nm.

3. Results and discussion

3.1. AC yield

The production yields of the prepared AC under OL and NA conditions were showed in Tables 2 and 3, respectively. As showed in Table 2, the AC yields in the carbonization temperature range of 400–800 °C were 36.3–24.5%. The yield decreased with increased final carbonization temperature because of the promotion of tar volatilization at higher temperatures [21]. Table 3 showed that the yield decreases as the impregnation ratio increased. This occurs because the higher impregnation ratio promoted the gasification of char and increased the total weight by excess chemicals [22]. The results obtained agreed with those of the study of Yorgun et al. [23], in which the yield of activated carbon decreased with increased of $ZnCl_2$ impregnation ratio.

3.2. The effect of the carbonization temperature

From Fig. 2(a), at low relative pressures, a rapid increase in the adsorption/desorption isotherms was observed in the curve of the sample prepared at 400 °C, which was followed by a nearly horizontal plateau at low relative pressures, indicating a type I isotherm based on the classification of Brunauer, Deming, Deming and Teller (BDDT) [24]. A type I isotherm represents a material with a microporous structure [23]. The other curves present a wide knee and a slope at higher relative pressures than 0.2, and all curves exhibited narrow

Table 2
Surface areas and pore volumes of activated carbons at various final carbonization temperatures (impregnation ratio = 100%).

Sample	S_{BET} (m^2/g)	V_T (cm^3/g)	V_{mi} (cm^3/g)	V_{me} (cm^3/g)	D_p (nm)	Yields (%)
AC-1	986	0.475	0.278	0.197	2.182	36.3
AC-2	1234	0.659	0.264	0.395	2.190	31.7
AC-3	1348	0.714	0.222	0.492	2.224	30.2
AC-4	1217	0.637	0.225	0.412	2.159	26.3
AC-5	1052	0.568	0.182	0.385	2.209	24.5

Table 3
Surface areas and pore volumes of activated carbons at various impregnation ratios (activated temperature = 600 °C).

Sample	S_{BET} (m^2/g)	V_T (cm^3/g)	V_{mi} (cm^3/g)	V_{me} (cm^3/g)	D_p (nm)	Yields (%)
AC-6	918	0.380	0.273	0.321	2.086	31.6
AC-3	1348	0.714	0.222	0.492	2.224	30.2
AC-7	1357	1.065	0.083	0.982	3.158	29.2
AC-8	1190	1.002	0.078	0.924	3.366	28.4
AC-9	1202	1.384	0.073	1.311	4.606	26.7

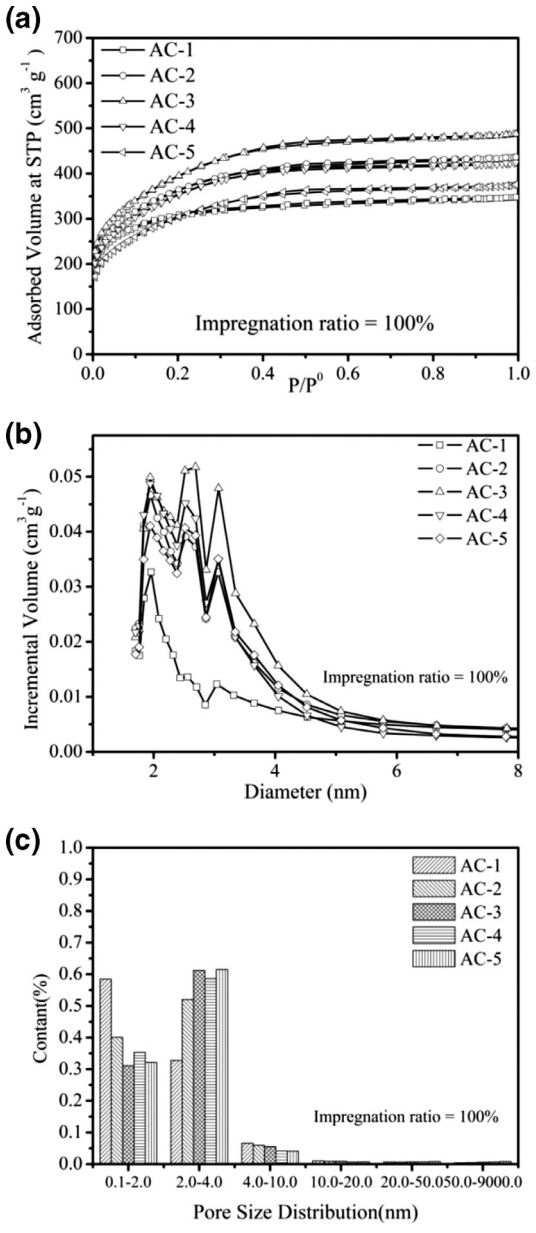

Fig. 2. N_2 adsorption and desorption isotherms at 77 K of samples prepared at various activation temperature under OL condition (a) and the pore-size distribution (b, c).

hysteresis loops, indicating the presence of mesoporosity [25]. The pore-size distributions of the AC with variable temperature were calculated by the BJH method and were showed in Fig. 2 (b) and (c). As can be observed in Fig. 2 (b), AC-1 showed a narrow pore-size distribution, indicating that the majority of the pores had a diameter of approximately 2 nm. The content of the pore-size distribution can be observed in Fig. 2 (c), which showed that AC-1 mainly had a microporous distribution. However, other samples showed similar pore-size distributions and more mesoporosity.

Table 2 listed the effects of the temperature on the physical properties of the AC. It can be seen that S_{BET} and V_T increased with the carbonization temperature from 400 to 600 °C and then gradually decreased with carbonization temperature from 600 to 800 °C. The maximum S_{BET} of 1348 m^2/g and the maximum V_T of 0.714 cm^3/g were obtained at 600 °C. Above 600 °C, $ZnCl_2$ does not work as an activation agent, and the surface area and pore volume decreased because of heat shrinkage [26]. However, with increased carbonization temperature, the average pore diameter changed slightly. For the DPR, when the activation temperature was above 400 °C, the N_2 adsorption/desorption isotherms and the pore-size distribution curves had similar tendencies, indicated that the carbonization temperature had a greater influence on the surface areas than the pore development.

3.3. The effect of the impregnation ratio

The impregnation ratio was the most decisive parameter in the chemical activation of DPR by $ZnCl_2$. Fig. 3(a) showed the N_2 adsorption/desorption isotherms of the AC with various impregnation ratios. It was obvious that the shapes of the N_2 adsorption/desorption isotherms gradually changed with increased impregnation ratios. The AC samples at low impregnation ratios of 50% exhibited a steep type I isotherm. The adsorption curve rose sharply at a relative pressure less than 0.1 and then approached a plateau with increased relative pressure, showed that the AC at this impregnation ratio was mainly microporous. As the impregnation ratio increased to 100%, it was obvious that a wide knee and a slope can be observed at relative pressures higher than 0.2, indicated the presence of mesoporosity. When the impregnation ratio increased to 150–250%, the increment of N_2 adsorption was significant in the higher relative pressure range, and samples AC-7 and AC-8 exhibited type IV isotherms with hysteresis loops of type H2, indicated the presence of a large amount of mesopores in the carbon corpuscular with poorly-defined pore shapes. Steep type IV isotherms with hysteresis loops of type H1 can also be observed in the AC-9 curves. This behavior suggested the presence of a large amount of mesopores in the samples prepared with high impregnation ratios.

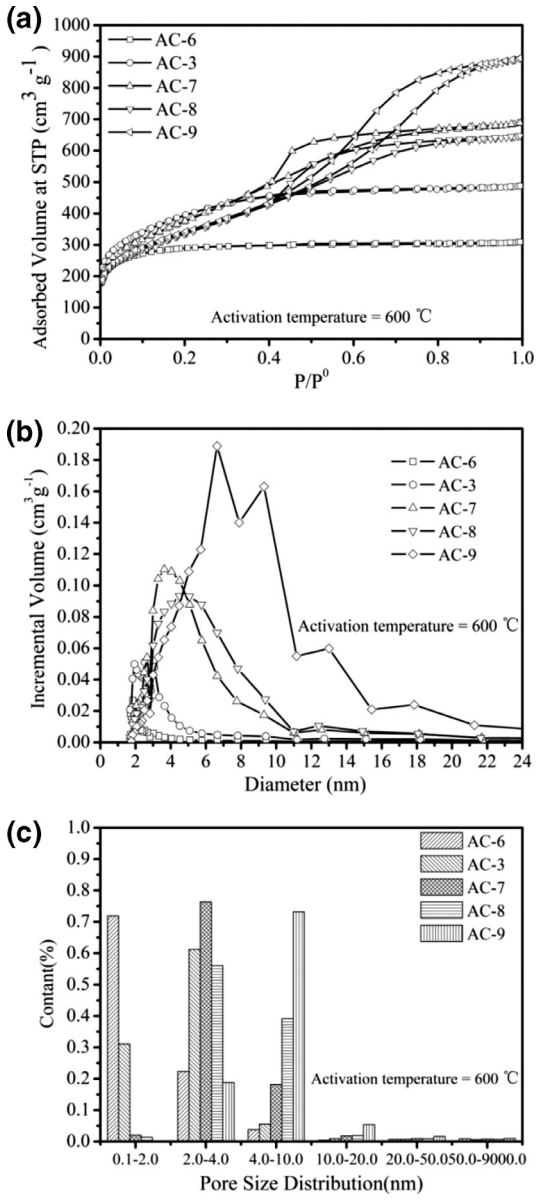

Fig. 3. N_2 adsorption and desorption isotherms at 77 K of samples prepared at various impregnation ratios under the OL condition (a) and pore-size distribution (b, c).

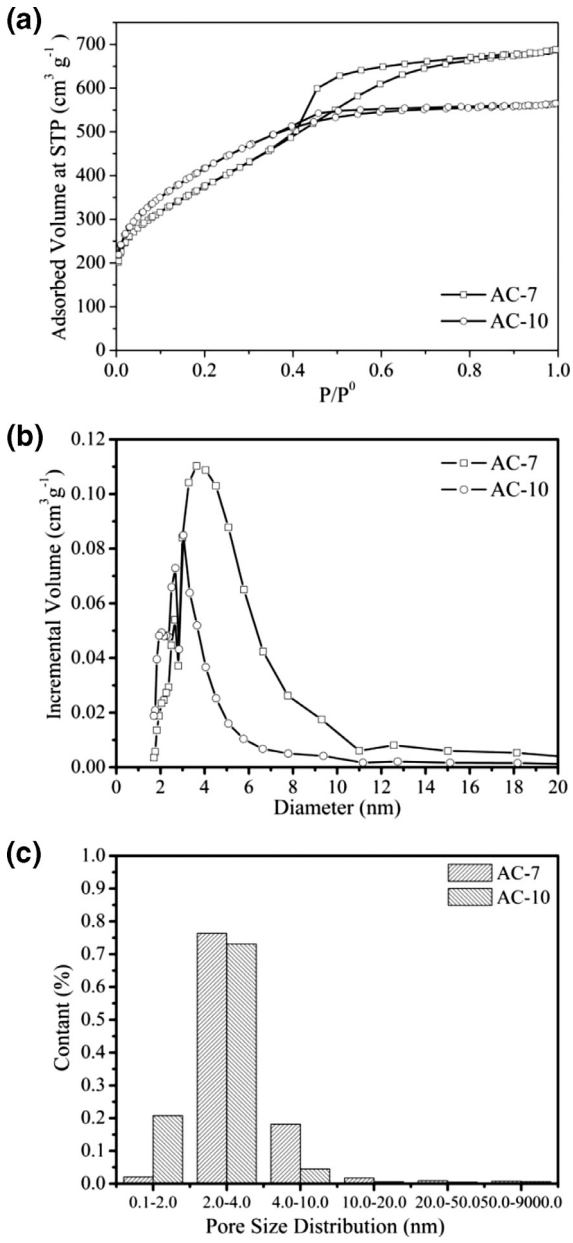

Fig. 4. N_2 adsorption and desorption isotherms at 77 K of samples prepared under the OL and NA conditions (a) and pore-size distribution (b, c).

The pore-size distributions of the AC with various impregnation ratios were determined by the BJH method and are shown in Fig. 3(b) and (c). It was obvious that the prepared carbon had a narrow, microporous pore-size distribution at an impregnation ratio of 50%, and the pore-size distribution became wider with increasing impregnation ratio. It can be observed that the pore size was mainly a microporous distribution at the impregnation ratio of 50%. The pore-size distributed at 2–4 nm with impregnation ratios ranging from 100% to 200% and the sample with the ratio of 150% had the highest pore-size distribution content. The pore size distribution at 4–10 nm was obtained for the sample with a ratio of 250%, which indicated that the impregnation ratio had a greater influence on the pore development than the surface areas.

The physical properties of the ACs were showed in Table 3. The S_{BET} of the AC increased rapidly with increasing impregnation ratio up to 150%. The maximum of S_{BET} was 1357 m^2/g. When the impregnation ratio was above 150%, S_{BET} decreased slightly. The values of V_T, V_{me} and D_p increased rapidly with increasing impregnation ratio, whereas V_{mi} decreased with the increasing ratio, for which the attack of the chemical was larger [27]. According to the obtained results, activated carbon with high surface areas (S_{BET}) and pore volumes (V_T, V_{mi}, and V_{me}) was obtained at a final impregnation ratio of 150%.

3.4. The effect of oxygen-limited conditions and N_2-atmosphere conditions

Fig. 4(a) showed the N_2 adsorption/desorption isotherms of the activated carbons prepared under OL and NA conditions. From Fig. 4(a), it can be seen that, under OL conditions, the increment of N_2 adsorption was significant in the higher relative pressure range. This suggests type IV isotherms with hysteresis loops of type H2. The curve of the sample prepared under NA conditions presented a wide knee and a slope and exhibited type I isotherms with small hysteresis loops of type H2. This occurs because the activated carbon prepared under OL conditions had greater mesoporosity and a wider pore size. The pore-size distributions showed in Fig. 4(b) and (c) support the results, confirming that the activated carbons obtained from the OL conditions have higher mesoporosity.

Table 4
Surface areas and pore volumes of activated carbons at OL and NA (activated temperature = 600 °C, impregnation ratio = 100%).

Sample	S_{BET} (m^2/g)	V_T (cm^3/g)	V_{mi} (cm^3/g)	V_{me} (cm^3/g)	D_p (nm)
AC-7	1357	1.065	0.083	0.982	3.158
AC-10	1485	0.875	0.189	0.656	2.355

Table 4 listed the physical properties of the AC prepared under OL and NA conditions. The results showed that the AC prepared under NA conditions had higher S_{BET} and V_{mi}, whereas the AC prepared under OL conditions had higher V_T and V_{me}. The possible explanation was that a small amount of oxygen could promote volatile-matter elimination and consume surface carbon, increased the pore volume and pore size, destroyed the microporous structure, and decreased the surface area. The result of the ultimate analysis (Table 1) showed that AC-7 had a lower C content, which also supported this assumption.

3.5. TG-DTG

To evaluate the behavior of the DPR as a function of the temperature, thermal analysis was performed in nitrogen atmosphere. To highlight the temperature at which a process involving a change of mass occurs, the differential curves (DTG) were also displayed in Fig. S1. Ahmadpour and Do [28] carbonized bituminous coal impregnated with $ZnCl_2$, and determined that hydrogen was evolved below 200 °C. When DPR with $ZnCl_2$ was carbonized in the temperature range from 150 to 250 °C, it was concluded that hydrogen was evolved. In the temperature range from 300 to 400 °C, the sample mass loss slowed. This showed that the evolution of the volatile matter was restricted by the impregnation of $ZnCl_2$. The volatile matter evolved in this temperature range was mainly tar [28,29]. It claimed that $ZnCl_2$ works as dehydration agent, and then it concluded that the dehydration induced the charring and aromatization of the carbon and restricted the formation of tar in this temperature range [26].

The sample mass decreased markedly in the temperature range from 450 to 600 °C. This was characterized by the decomposition of DPR and the restriction of $ZnCl_2$ evaporation. Nevertheless, above 600 °C, no significant weight loss was observed because $ZnCl_2$ works effectively only below a temperature of 600 °C [26], and therefore, a temperature of 600 °C could be selected for preparation of the activated carbon.

3.6. XRD

Fig. S2 showed the XRD patterns of the DPR and AC obtained from $ZnCl_2$ activation under various reaction conditions. In the DPR, a broad peak appearing at $2\theta = 21.8°$ was attributed to the characteristic crystal structure of cellulose [10]. The peak disappeared after carbonization due to the decomposition of the cellulose. Two broad peaks appeared at approximately $2\theta = 25°$ and 43° after activation with $ZnCl_2$ in AC-7 and AC-10, respectively. They corresponded to the formation of hexagonal graphite structures (0 0 2) and (1 0 0) (overlapped 1 0 0 and 1 0 1). The calculated d0 0 2 values for AC-7 and AC-10 were 0.383 and 0.373 nm higher than that of graphite (0.335 nm), respectively. The results demonstrated a turbostratic carbon structure with randomly oriented graphitic carbon layers [30]. The peaks at $2\theta =$ 43° were due to the creation of pores by the decomposition of carbon along the direction of the graphic structures [31].

3.7. Surface chemistry characterization

Fig. S3 showed the FTIR spectrum of the DPR in the range of 400 to 4000 cm^{-1}. The bands at 3424 cm^{-1} (DPR) were O—H stretching in the hydroxyl functional groups. The bands at 2924 cm^{-1} indicated the presence of an aliphatic —CH stretching. A medium band at 1737 cm^{-1} was C=O stretching, an indication of the presence of an aldehyde in DPR [32]. The band at 1649 cm^{-1} may be due to the stretching vibrations of C=C bonds in olefinic structures [33]. Two bands at approximately 1537 and 1512 cm^{-1} were attributed to the skeletal C=C vibrations in the aromatic rings. The band at 1457 cm^{-1} was attributed to a symmetrical angular deformation on the plane of the methylene groups. The band at 1246 cm^{-1} and a relatively intense band at approximately 1078 cm^{-1} can be assigned to C—O stretching vibrations in alcohol, phenol, ether or ester groups. From the band assignment, the oxygen-containing groups presented in the DPR include carbonyl groups, ethers, esters, alcohols, and phenol groups.

Fig. S3 also showed that the FTIR spectra of AC-7 and AC-10 were similar. Fewer functional groups were detected on the ACs, indicating that the surface functional groups of DPR have been significantly changed under OL and NA conditions. Compared with the DPR, the C—H vibrations in the methyl and methylene groups (at 2924 cm^{-1}) became much weaker after activation, suggested the carbonization of the material was almost complete.

3.8. SEM

To observe the morphology of the prepared samples, the SEMs of DPR, AC-7 and AC-10 were presented in Fig. S4. Fig. S4(a) presents the micrograph for the DPR sample. The surface of the DPR was smooth without porous characteristics (Fig. S4(a)). Nevertheless, major surface damage appeared when the DPR was carbonized, due to the release of volatile compounds. The micrographs showed in Fig. S4(b)–(c) and (d)–(e) correspond to the materials collected after the activation process with $ZnCl_2$ under OL and NA conditions, respectively. Two activated carbon samples showed that the porous characteristics were generated after the activation, which contributes to the increase of the surface area.

3.9. Zeta potential

To obtain information about the surface charge of these materials, zeta potential measurements were performed at various pH values, as shown in Table S1, using variable amounts of 0.1 M NaOH and 0.1 M HCl to adjust the pH of the samples. The zeta potentials of AC-7 and AC-10 became negative with increasing suspension pH, and those for AC-7 were more negative than those for AC-10 at a higher pH value, which may be attributed to the fact that more oxygen-containing functional groups (*e.g.*, —COOH and —OH) were located at the surface of the activated carbon prepared by the oxygen-limited condition. The ultimate analyses correspond to this assumption (Table 1). With increasing pH value, the dissociation of these organic functional groups increased, and hence the ability to interact electrostatically with the positive charge increased.

3.10. MB adsorption tests

The adsorption capacity of the ACs was tested using MB as a representative pollutant. The adsorption isotherms for MB were showed in Fig. S5. The carbon activated under OL and NA conditions presented a superior adsorption capacity, approximately 539.3 and 545.8 mg/g, respectively. In contrast, the adsorption capacity under various activation conditions showed little difference. Therefore, the AC from DPR had an excellent adsorption capacity, and so it can be used in wastewater treatment.

4. Conclusions

DPR was used as a raw material to prepare activated carbon by a chemical activation method using $ZnCl_2$. The AC formed under OL conditions had a larger V_t than that formed under NA conditions. For sample AC-7, the S_{BET} and V_T were as high as 1357 m^2/g and

1.065 cm^3/g, respectively. The adsorption test showed that the AC had a high MB adsorption capacity. Therefore, DPR was a potential precursor material for the production of AC.

Acknowledgments

This work was financially supported by Natural Science Foundation of China (21174114), the Program for Changjiang Scholars and the Innovative Research Team in the University (IRT1177) and the Program for Gansu Innovation Group (1208RJYA055). We also thank Key Laboratory of Eco-Environment-Related Polymer Materials (Northwest Normal University), Ministry of Education, for financial support. We also acknowledge Professor Hao-hao Huang for careful revisions.

Supplementary materials

Supplementary material associated with this article can be found, in the online version, at doi:10.1016/j.jtice.2014.11.024.

References

[1] Kyzas GZ, Kostoglou M. Green adsorbents for wastewaters: a critical review. Materials 2014;7:333–64.
[2] Chen Y, Zhai SR, Liu N, Song Y, An QD, Song XW. Dye removal of activated carbons prepared from NaOH-pretreated rice husks by low-temperature solution-processed carbonization and H_3PO_4 activation. Bioresour Technol 2013;144:401–9.
[3] Jiang J, Xu RK, Jiang TY, Li Z. Immobilization of Cu(II), Pb(II) and Cd(II) by the addition of rice straw derived biochar to a simulated polluted Ultisol. J Hazard Mater 2012;229–230:145–50.
[4] Gurten II, Ozmak M, Yagmur E, Aktas Z. Preparation and characterisation of activated carbon from waste tea using K_2CO_3. Biomass Bioenergy 2012;37:73–81.
[5] Hjaila K, Baccar R, Sarrà M, Gasol CM, Blánquez P. Environmental impact associated with activated carbon preparation from olive-waste cake via life cycle assessment. J Environ Manage 2013;130:242–7.
[6] Gonçalves M, Guerreiro MC, Oliveira LCA, Castro CS. A friendly environmental material: iron oxide dispersed over activated carbon from coffee husk for organic pollutants removal. J Environ Manage 2013;127:206–11.
[7] Loredo-Cancino M, Soto-Regalado E, Cerino-Córdova FJ, García-Reyes RB, García-León AM, Garza-González MT. Determining optimal conditions to produce activated carbon from barley husks using single or dual optimization. J Environ Manage 2013;125:117–25.
[8] Hamdaoui O. Batch study of liquid-phase adsorption of methylene blue using cedar sawdust and crushed brick. J Hazard Mater 2006;135:264–73.
[9] Williams PT, Reed AR. Development of activated carbon pore structure via physical and chemical activation of biomass fibre waste. Biomass Bioenergy 2006;30:144–52.
[10] Regmi P, Moscoso JLG, Kumar S, Cao XY, Mao JD, Schafran G. Removal of copper and cadmium from aqueous solution using switchgrass biochar produced via hydrothermal carbonization process. J Environ Manage 2012;109:61–9.
[11] Wang LG. Application of activated carbon derived from 'waste' bamboo culms for the adsorption of azo disperse dye: kinetic, equilibrium and thermodynamic studies. J Environ Manage 2012;102:79–87.
[12] Arami-Niya A, Daud WMAW, Mjalli FS. Using granular activated carbon prepared from oil palm shell by $ZnCl_2$ and physical activation for methane adsorption. J Anal Appl Pyrol 2010;89:197–203.
[13] Rafatullah M, Sulaiman O, Hashim R, Ahmad A. Adsorption of methylene blue on low-cost adsorbents: a review. J Hazard Mater 2010;177:70–80.
[14] Obidziński S. Analysis of usability of potato pulp as solid fuel. Fuel Process Technol 2012;94:67–74.
[15] Bengtsson H, Montelius C, Tornberg E. Heat-treated and homogenised potato pulp suspensions as additives in low-fat sausages. Meat Sci 2011;88:75–81.
[16] Mayer F. Potato pulp: properties, physical modification and applications. Polym Degrad Stabil 1998;59:231–5.
[17] Chen BL, Zhou DD, Zhu LZ. Transitional adsorption and partition of nonpolar and polar aromatic contaminants by biochars of pine needles with different pyrolytic temperatures. Environ Sci Technol 2008;42:5137–43.
[18] Brunauer S, Emmett PH, Teller E. Adsorption of gases in multimolecular layers. J Am Chem Soc 1938;60:309–19.
[19] Barrett EP, Joyner LG, Halenda PP. The determination of pore volume and area distributions in porous substance. I. computations from nitrogen isotherms. J Am Chem Soc 1951;73:373–80.
[20] Oh GH, Park CR. Preparation and characteristics of rice-straw-based porous carbons with high adsorption capacity. Fuel 2002;81:327–36.
[21] Qian QR, Machida M, Tatsumoto H. Preparation of activated carbons from cattle-manure compost by zinc chloride activation. Bioresour Technol 2007;98:353–60.
[22] Kılıç M, Apaydın-Varol E, Pütün AE. Preparation and surface characterization of activated carbons from Euphorbia rigida by chemical activation with $ZnCl_2$, K_2CO_3, NaOH and H_3PO_4. Appl Surf Sci 2012;261:247–54.
[23] Yorgun S, Vural N, Demiral H. Preparation of high-surface area activated carbons from Paulownia wood by $ZnCl_2$ activation. Micropor Mesopor Mater 2009;122:189–94.
[24] Brunauer S, Deming LS, Deming WE, Teller E. On a theory of the van der Waals adsorption of gases. J Am Chem Soc 1940;62:1723–32.
[25] Lillo-Ródenas MA, Cazorla-Amorós D, Linares-Solano A. Behaviour of activated carbons with different pore size distributions and surface oxygen groups for benzene and toluene adsorption at low concentrations. Carbon 2005;43:1758–67.
[26] Hayashi J, Kazehaya A, Muroyama K, Watkinson AP. Preparation of activated carbon from lignin by chemical activation. Carbon 2000;38:1873–8.
[27] Molina-Sabio M, Rodríguez-Reinoso F. Role of chemical activation in the development of carbon porosity. Colloid Surf A 2004;241:15–25.
[28] Ahmadpour A, Do DD. The preparation of activated carbons from coal by chemical and physical activation. Carbon 1996;34:471–9.
[29] Rodríguez-Reinoso F, Molina-Sabio M. Activated carbons from lignocellulosic materials by chemical and/or physical activation: an overview. Carbon 1992;30:1111–18.
[30] Wang TH, Tan SX, Liang CH. Preparation and characterization of activated carbon from wood *via* microwave-induced $ZnCl_2$ activation. Carbon 2009;47:1880–3.
[31] Kennedy LJ, Vijaya JJ, Sekaran G. Effect of two-stage process on the preparation and characterization of porous carbon composite from rice husk by phosphoric acid activation. Ind Eng Chem Res 2004;43:1832–8.
[32] Deng H, Lu JJ, Li GX, Zhang GL, Wang XG. Adsorption of methylene blue on adsorbent materials produced from cotton stalk. Chem Eng J 2011;172:326–34.
[33] Liou TH. Development of mesoporous structure and high adsorption capacity of biomass-based activated carbon by phosphoric acid and zinc chloride activation. Chem Eng J 2010;158:129–42.